



A novel strategy for synthesis of hollow gold nanosphere and its application in electrogenerated chemiluminescence glucose biosensor



Xia Zhong, Ya-Qin Chai*, Ruo Yuan*

Key Laboratory of Luminescence and Real-time Analysis Chemistry, Ministry of Education, College of Chemistry and Chemical Engineering, Southwest University, Chongqing 400715, PR China

ARTICLE INFO

Article history:

Received 13 December 2013

Received in revised form

21 March 2014

Accepted 29 March 2014

Available online 4 April 2014

Keywords:

Electrogenerated chemiluminescence

Glutaraldehyde

Glucose oxidase

Nanospheres

Glucose

ABSTRACT

Well-distributed hollow gold nanospheres ($\text{Au}_{\text{shell}}@GOD$) (20 ± 5 nm) were synthesized using the glucose oxidase (GOD) cross-linked with glutaraldehyde as a template. A glucose biosensor was prepared based on $\text{Au}_{\text{shell}}@GOD$ nanospheres for catalyzing luminol electrogenerated chemiluminescence (ECL). Firstly, chitosan was modified in a glassy carbon electrode which offered an interface of abundant amino-groups to assemble $\text{Au}_{\text{shell}}@GOD$ nanospheres. Then, glucose oxidase was adsorbed on the surface of $\text{Au}_{\text{shell}}@GOD$ nanospheres via binding interactions between Au_{shell} and amino groups of GOD to construct a glucose biosensor. The $\text{Au}_{\text{shell}}@GOD$ nanospheres were investigated with TEM and UV–vis. The ECL behaviors of the biosensor were also investigated. Results showed that, the obtained $\text{Au}_{\text{shell}}@GOD$ nanospheres exhibited excellent catalytic effect towards the ECL of luminol- H_2O_2 system. The response of the prepared biosensor to glucose was linear with the glucose concentration in the range of 1.0 μM to 4.3 mM ($R=0.9923$) with a detection limit of 0.3 μM (signal to noise=3). This ECL biosensor exhibited short response time and excellent stability for glucose. At the same time the prepared ECL biosensor showed good reproducibility, sensitivity and selectivity.

© 2014 Elsevier B.V. All rights reserved.

1. Introduction

Electrogenerated chemiluminescence (also known as electrochemiluminescence) is the combination electrochemistry and chemiluminescence, which not only possesses the advantages of electrochemical analysis, but also exhibits many characteristics of chemiluminescence analysis [1]. As a new electrochemical detection technology, electrogenerated chemiluminescence (ECL) is of interest to researchers due to its versatility, simplified optical set-up, low background signal and high sensitivity. Electrogenerated chemiluminescence signals are usually obtained from the excited states of a luminophore generated at the electrode surface during the electrochemical reaction [2]. Electrogenerated chemiluminescence technology has been widely applied in the field of biotechnology, food safety and clinical diagnosis [3–5]. In recent years, some enzyme biosensors based on electrogenerated chemiluminescence also have been reported for detecting glucose, alcohol, hypoxanthine, cholesterol, choline, etc. [6–10].

Luminol (2,3-aminophthalhydrazide) has been widely used in constructing electrogenerated chemiluminescence systems because

of its low oxidation potential, inexpensive reagent consumption and the high emission yields [11–13]. The electrogenerated chemiluminescence of luminol can be triggered by applying an appropriate positive potential to the working electrode in the presence of hydrogen peroxide (H_2O_2) [1,9]. Some enzymes can produce H_2O_2 during their substrate-specific enzymatic reaction. The intensity of the electrogenerated chemiluminescence signal is directly proportional to the concentration of H_2O_2 which was generated by enzymatic catalysis. Therefore, a sensitive electrogenerated chemiluminescence glucose biosensor could be designed for measurement of glucose by detecting H_2O_2 indirectly [14,15].

Some nanomaterials such as gold nanoparticles (AuNPs) [9,16], platinum nanoparticles [14], palladium nanoparticles [16], graphene [17], TiO_2 nanocrystals [18] and quantum dots [19] have been used in the electrogenerated chemiluminescence system. Among these nanomaterials, gold nanoparticles have excellent catalytic performance to directly enhance the electrogenerated chemiluminescence intensity of luminol- H_2O_2 system [20–22]. So, gold nanoparticles can be used as the immobilization matrix for the design of a novel biosensor with enhanced analytical performance. A lot of hollow capsules nanoparticles have been synthesized and applied [23–26]. Sharma's group [27] has obtained hollow gold nanoparticles by leaching out silver chloride (AgCl) from $\text{Au}_{\text{shell}}@AgCl_{\text{core}}$ nanoparticles with dilute ammonia solution, Jiang's group [28] has synthesized Polystyrene/gold core-shell

* Corresponding authors. Tel.: +86 23 6825 2277; fax: +86 23 6825 4000.

E-mail addresses: yqchai@swu.edu.cn (Y.-Q. Chai), yuanruo@swu.edu.cn (R. Yuan).

nanocomposites based on the method of ionic self-assembly and the *in situ* reduction. These preparation process of hollow gold nanoparticles were complicated.

Herein, the aim of this work is to synthesize well-distributed hollow gold nanospheres encapsulating GOD ($\text{Au}_{\text{shell}}\text{@GOD}$) (about 20 ± 5 nm) in a simple way and develop an ECL biosensor. The prepared hollow $\text{Au}_{\text{shell}}\text{@GOD}$ nanoparticles have large surface area, high conductivity, good biocompatibility, which could effectively increase the loading of GOD and keep the biological activity of GOD. Thus, GOD molecules can exist inside and outside of the Au_{shell} , which could effectively amplify the ECL intensity of luminol- H_2O_2 system. In addition, the Au_{shell} assembling on the electrode can catalyze the electro-oxidation of luminol, and the more strong ECL signal was obtained in neutral aqueous solution. Such fabrication of biosensor exhibited short response time and excellent stability for glucose detecting. At the same time the prepared ECL biosensor showed good reproducibility, sensitivity and selectivity.

2. Experimental

2.1. Reagents and materials

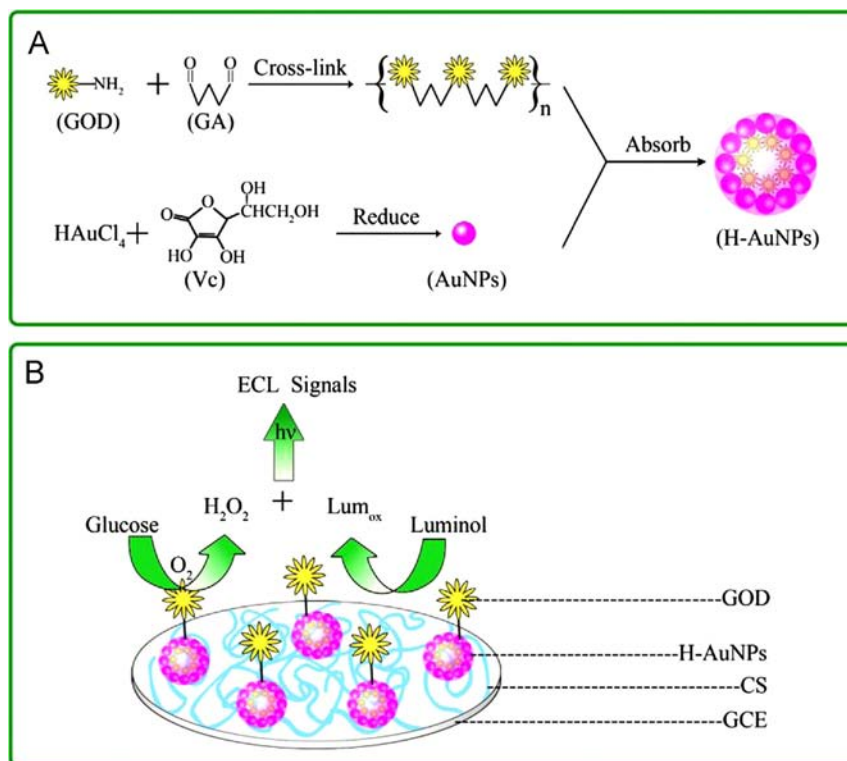
GOD and chitosan (CS) were obtained from Sigma Chemical Co. (St. Louis, MO, USA). Gold chloride tetrahydrate ($\text{HAuCl}_4 \cdot 4\text{H}_2\text{O}$) was obtained from Sinopharm Chemical Reagent Co. Ltd. (Shanghai, China). Glutaraldehyde (GA) was purchased from Beijing Chemical Reagent Co. (Beijing, China). L-ascorbic acid (AA) was purchased from Boyi Chemical Reagent Co. (Chongqing, China). Phosphate buffer solutions (PBS) with various pH values were prepared with 0.1 M KH_2PO_4 and 0.1 M Na_2HPO_4 . The supporting electrolyte was 0.1 M KCl. All chemicals were analytical grade and were used as received without further purification. Ultrapure water was used throughout all experiments.

2.2. Apparatus

The ECL emission was measured using a model MPI-A electrochemiluminescence analyzer (Xi'an Remax Electronic Science & Technology Co. Ltd., China) with the voltage of the photomultiplier tube (PMT) set at 600 V in the detection process. Cyclic voltammetry (CV) was performed with a CHI 600D electrochemical workstation (Shanghai CH Instruments Co., China). All experiments were performed with a conventional three-electrode system including a bare or modified glassy carbon electrode (GCE, $\phi=4$ mm) as working electrode, a platinum wire as auxiliary electrode and a saturated calomel electrode (SCE) as reference electrode for electrochemical experiments, or Ag/AgCl electrode as a reference electrode for ECL experiments. The morphologies of the prepared $\text{Au}_{\text{shell}}\text{@GOD}$ were tracked by transmission electron microscopy (TEM, H600, Hitachi Instrument, Japan).

2.3. Preparation of hollow gold nanospheres encapsulating GOD ($\text{Au}_{\text{shell}}\text{@GOD}$)

The hollow gold nanospheres encapsulating GOD were synthesized using GOD cross-linked with glutaraldehyde as a template. Briefly, GOD cross-linked with glutaraldehyde was obtained by mixing 1.0 mL of 2 mg L^{-1} GOD solutions (pH 7.0) with 1.0 mL of 1.0% glutaraldehyde solution. Then, the mixture solution was placed in a refrigerator at 4°C for 12 h. Subsequently, 0.5 mL of above mixture solution and $100 \mu\text{L}$ of 1.0% gold chloride tetrahydrate were added in 5.0 mL ultrapure water with stirring. Afterward, 0.01 M ascorbic acid (AA) was injected into the solution with droplet under agitation, and the color of solution changed to claret. In the GOD-glutaraldehyde network structure, AuCl_4^- can be reduced by ascorbic acid to elemental Au that could grow into hollow gold nanospheres ($\text{Au}_{\text{shell}}\text{@GOD}$) in control. The morphology of $\text{Au}_{\text{shell}}\text{@GOD}$ was measured by TEM. The schematic diagram of the stepwise procedure of the synthesis is illustrated in Scheme 1(A).

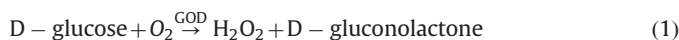


Scheme 1. (A) Synthesized process of hollow gold nanospheres ($\text{Au}_{\text{shell}}\text{@GOD}$); (B) Schematic description of response mechanism.

2.4. Fabrication of the ECL biosensor

A glassy carbon electrode was polished with 0.3 and 0.05 μm alumina slurry to gain a slick surface, and then was ultrasonically cleaned in ethanol and water drastically. Then it was dried at room temperature. Following this pretreatment, 10 μl of CS aqueous dispersion (1.0 mg mL^{-1}) was dropped on cleaned GCE. Then it was allowed to dry at room temperature in air. Subsequently, it was immersed in $\text{Au}_{\text{shell}}@GOD$ solution for 8 h to obtain $\text{Au}_{\text{shell}}@GOD/CS/GCE$. Afterward, the $\text{Au}_{\text{shell}}@GOD/CS/GCE$ was immersed in GOD solution (2 mg mL^{-1} in PBS, pH 7.0) for another 8 h to fabricate the $GOD/\text{Au}_{\text{shell}}@GOD/CS/GCE$. The modified process is schematically shown in Scheme 1(B). The biosensor was stored at 4°C in a refrigerator when not in use.

The probable principle of this biosensor related to the detection of glucose is also schematically shown in Scheme 1(B). The glucose in the solution reacts with the dissolved oxygen (O_2) in the presence of GOD to generate gluconolactone and H_2O_2 (Eq. (1)). Under positive potential and with the help of Au_{shell} , the luminol radical anion reacts with H_2O_2 , the product of the enzymatic reaction of GOD and glucose, at the electrode surface to produce the excited state 3-aminophthalate anion, which emits an ECL emission at 425 nm (Eq. (2)). The intensity of the ECL signal is directly proportional to the concentration of H_2O_2 which was produced by GOD and glucose. Therefore, a sensitive ECL glucose sensor could be developed for the detection of glucose by detecting H_2O_2 indirectly. Based on this principle, an ECL biosensor for glucose could be fabricated.



2.5. Measurement procedure

The prepared biosensor was placed in an ECL detector cell containing 3 mL PBS with 0.1 mM luminol and different concentration of glucose to record the change of ECL signals at room temperature. The voltage of the photomultiplier tube (PMT) was set at 600 V and the applied potential was 0.2–0.8 V (*vs.* Ag/AgCl) with a scan rate of 100 mV s^{-1} in the process of detection. On increasing the glucose concentration, the ECL signals of luminol enhanced. Therefore, the changes of ECL intensity directly connected with the concentration changes of glucose.

3. Results and discussion

3.1. Characterization of the $\text{Au}_{\text{shell}}@GOD$ nanoparticles

TEM technique was employed to confirm the successful synthesis of the hollow nanoparticles. A typical TEM image of $\text{Au}_{\text{shell}}@GOD$ is shown in Fig. 1(A). The photograph shows that well-dispersed $\text{Au}_{\text{shell}}@GOD$ are a hollow spherical with a mean size about $20 \pm 5 \text{ nm}$.

UV–vis absorption spectroscopy was used to further characterize the component of the hollow nanoparticles. The UV–vis absorption spectra of the $\text{Au}_{\text{shell}}@GOD$ colloidal solutions present a well-defined absorption band with a maximum at the wavelength $\lambda_{\text{max}} = 527 \text{ nm}$ (Fig. 1(B)). The AuNPs are known to have an intense Plasmon absorption band in this region [29]. Therefore, the absorption band at 527 nm arises from surface plasmon absorption of $\text{Au}_{\text{shell}}@GOD$. As expected, the results show that the prepared hollow $\text{Au}_{\text{shell}}@GOD$ was successfully prepared.

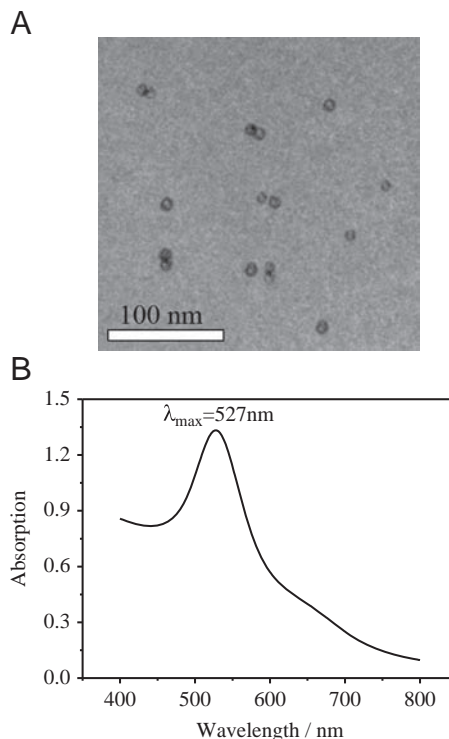


Fig. 1. (A) TEM images of $\text{Au}_{\text{shell}}@GOD$ nanoparticles (mode: Microprobe, voltage: 80 KV and current: 12.23 μA); and (B) UV-vis spectra of hollow $\text{Au}_{\text{shell}}@GOD$ nanoparticles.

3.2. Electrochemical impedance spectroscopy (EIS) and cyclic voltammetry (CV) characterization of the enzyme electrode

EIS was used to estimate the interfacial changes of the electrode. The semicircle diameter of impedance equals the electron transfer resistance (R_{et}), which lies on the electron transfer kinetics of the redox probe at the electrode interface. Fig. 2(A) shows the impedance spectrum of the modified electrode at different stages in 5.0 mM $\text{K}_3\text{Fe}(\text{CN})_6/\text{K}_4\text{Fe}(\text{CN})_6(1:1)$ solution (0.1 M KCl). The Nyquist semicircle of the CS/GCE (curve b) increased dramatically when compared with the bare GCE (curve a), which indicated that CS was fabricated on the GCE. However, when hollow $\text{Au}_{\text{shell}}@GOD$ was adsorbed on the electrode, the Nyquist semicircle decreased markedly (curve c) for the reason that hollow $\text{Au}_{\text{shell}}@GOD$ could facilitate electron transfer between solution and electrode surface. When the GOD was adsorbed on $\text{Au}_{\text{shell}}@GOD$ nanoparticles of the electrode (curve d), the Nyquist semicircle increased which may be caused by the hindrance of non-conductive GOD. For the sake of giving more detailed information about the impedance of the modified electrode, a modified Randles equivalent circuit (Fig. 2(A) insert) was chosen to fit the measured results.

The assembly process was also affirmed by CV in the potential range of -0.3 to 0.7 V in 5.0 mM $\text{K}_3\text{Fe}(\text{CN})_6/\text{K}_4\text{Fe}(\text{CN})_6(1:1)$ solution (0.1 M KCl) (Fig. 2(B)). The peak current and the peak-to-peak potential distance (ΔE) of the CV curves also revealed information about the electron-transfer process. As shown in Fig. 2(B), stable and well-defined redox peaks at 0.15 and 0.28 V at a scan rate of 50 mV/s were observed at bare GCE (curve a). The peak to peak separation (ΔE) is 0.13 V. When CS was deposited on GCE surface, the resulting electrode showed redox peaks at 0.04 V and 0.39 V and the $\Delta E = 0.35 \text{ V}$ (curve b). But an obvious decrease of peak current was noticed, which was attributed to the CS blocking the redox of the electrode surface. In comparison with curve b, the

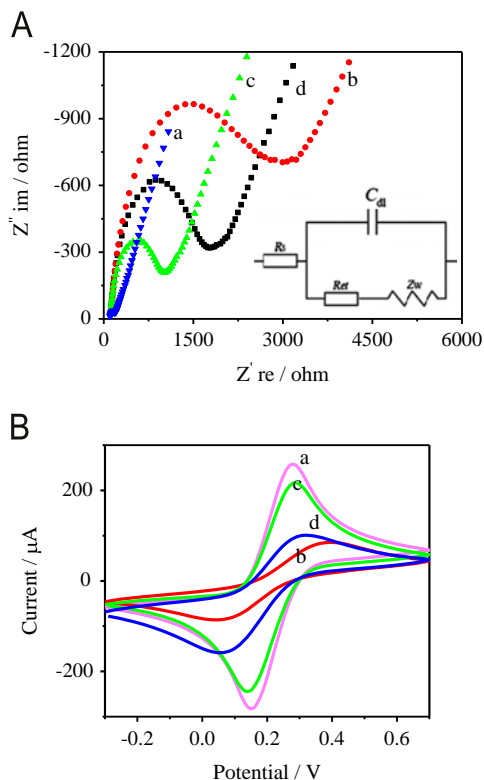


Fig. 2. EIS (A) and CVs (B) of different electrodes (a) bare GCE, (b) CS/GCE, (c) Au_{shell}@GOD/CS/GCE, and (d) GOD/Au_{shell}@GOD/CS/GCE in 5.0 mM [Fe(CN)₆]^{4−/3−} solution (containing 0.1 M KCl) at a scan rate of 100 mV/s. Inset (A): equivalent circuit adopted to fit the impedance data, (1) R_s (electrolyte resistance); (2) Z_w (Warburg impedance); (3) R_{et} (electron-transfer resistance); (4) C_{dl} (double-layer capacitance).

peak currents increased and $\Delta E=0.15$ V after loading hollow Au_{shell}@GOD, which contributed to the fact that nanoparticles can promote the transmission of electrons (curve c). However, after the second layer GOD were modified onto the electrode via binding interactions between nanoparticles and amino groups of GOD, a further decrease in peak current was observed and $\Delta E=0.27$ V (curve d). The conclusions of CV are confirmed with EIS. The above results could clearly confirm the successful assembled the biosensor.

The effect of variation of scan rate on electrochemical behavior of [Fe(CN)₆]^{3−/4−} (5.0 mM) in KCl aqueous solution (0.1 M) was investigated. The variation of peak current (i_p) with the square root of scan rate ($\nu^{1/2}$) was found to be linear in the investigated scan rate range of 10–300 mV/s, demonstrating that the electrochemical process is diffusion-controlled. The diffusion coefficient was 1.0×10^{-5} cm² s^{−1}.

3.3. Optimum conditions of the biosensor

In order to obtain the optimum performance of the prepared ECL biosensor for glucose, the concentrations of luminol in solution and adsorbing time of hollow Au_{shell}@GOD with CS in electrode were studied. The result showed that the ECL intensity increased with the increase of luminol concentration, which may be because the ECL intensity is directly proportional to the quantity of luminol. Consideration of the ECL intensity and sensitivity of the glucose biosensor, herein, 0.1 mM was selected as the optimal concentration of luminol for the optimum concentration. The adsorbing amount of Au_{shell}@GOD could also influence the intensity of the ECL signal. As a result, the optimum adsorbing time is 8 h which selected for the biosensor fabrication.

In order to obtain a better ECL response to glucose, the effect of medium pH on the biosensor was investigated. In this ECL system, the pH of PBS will influence the enzyme activity and ECL signal intensity. As we know, luminol generates strong chemiluminescence or ECL signals in alkaline media. However, enzyme could not maintain its biological activity in alkaline media. Considering the pH of human blood is about 7.4 and GOD can keep its activity in this pH condition. In this case, pH 7.4 was selected to ensure sensitivity and stability of the sensor.

3.4. Performance of the biosensor

The ECL response of the glucose biosensor was investigated with the ECL technique under optimal experimental conditions. A comparative study was carried out by using two kinds of biosensor (Fig. 3): Au_{shell}@GOD/CS/GCE (A) and GOD/Au_{shell}@GOD/CS/GCE (B). With the increasing concentration of glucose, the ECL intensity of the two kinds of biosensor is increased. The inset displays the calibration plots of the two kinds of sensor for glucose determination. For Au_{shell}@GOD/CS/GCE, the ECL signals linearly increases in the range of 10 μM–3.28 mM, with a detection limit of 3 μM at the signal-to-noise ratio of 3. The regression equation was I (a.u.) = $0.229 \times 10^3 c$ (mM) + 102.06 with a correlation coefficient of 0.9913. The result showed the GOD inside of Au_{shell}@GOD still have its biological activity and can oxidize glucose to produce H₂O₂. The intensity of the ECL signal is directly proportional to the concentration of H₂O₂ which was produced by GOD and glucose. For GOD/Au_{shell}@GOD/CS/GCE, the ECL signals increased linearly in the range of 1.0 μM–4.3 mM with a detection

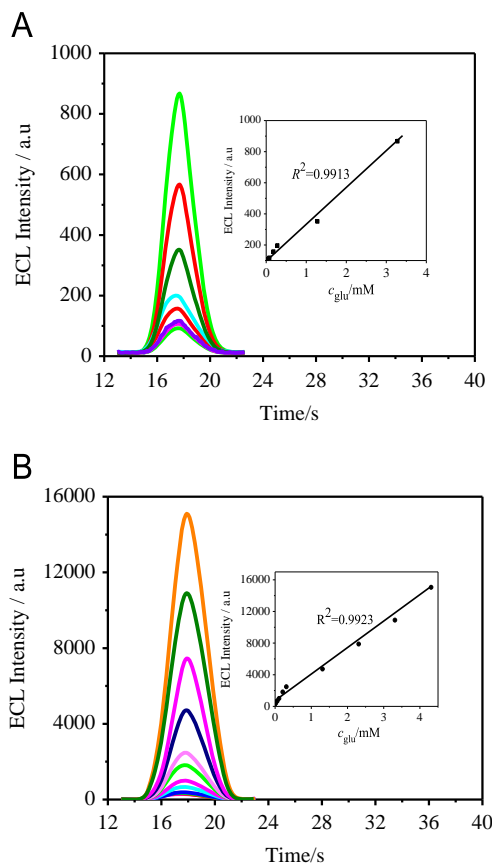


Fig. 3. ECL responses of Au_{shell}@GOD/CS/GCE (A) in the presence of 0.01, 0.02, 0.08, 0.18, 0.28, 1.28, and 3.28 mM glucose; and GOD/Au_{shell}@GOD/CS/GCE (B) in the presence of 0.001 mM, 0.005, 0.01, 0.06, 0.11, 0.21, 0.31, 1.31, 2.31, 3.31 and 4.31 mM glucose in pH 7.4 PBS with 0.1 mM luminol. Inset showed linear relationship between the ECL signal intensity and the concentration of glucose.

limit of 0.3 μM at the signal-to-noise ratio of 3. The regression equation was $I(\text{a.u.}) = 3.24 \times 10^3 c (\text{mM}) + 617.78$ with a correlation coefficient of 0.9923. Compared with Fig. 3(A) the slope of GOD/Au_{shell}@GOD/CS/GCE is higher than the Au_{shell}@GOD/CS/GCE that maybe own to the additional absorbing GOD outside of Au_{shell}, which can oxidize glucose with the dissolved oxygen (O₂) in the solution to form gluconolactone and produce more H₂O₂. Under positive potential and with the help of nanoparticles, the luminol radical anion can quickly react with those H₂O₂ and arise the excited state 3-aminophthalate anion to emit the stronger ECL emission.

This glucose biosensor exhibited good performance due to the following reasons: (i) the GOD inside of Au_{shell}@GOD still had its biological activity and Au_{shell}@GOD nanoparticle had high surface-to-volume ratio, good biocompatibility that can absorb more enzyme outside the Au_{shell}. (ii) The Au_{shell}@GOD nanoparticles assembled on the electrode could catalyze the electro-oxidization of luminol, and thus enhance the ECL intensity of luminol-H₂O₂ system. (iii) ECL technique has the advantages of electrochemical and luminescent techniques, such as low background disturbance, good temporal and spatial control, high sensitivity, low detection limit and so on.

3.5. Stability, reproducibility and interferences of the biosensor

The reproducibility and repeatability of the sensors were performed by three assaying electrodes prepared in the same condition. A relative standard deviation (R.S.D.) was 3.9% in the presence of 0.5 mM glucose solution. A single sensor was successively tested ($n=22$) in the presence of 3.3 mM glucose (Fig. 4) with a R.S.D. of 0.8%

The stability of biosensor was also the tested by monitoring its ECL response towards glucose. The prepared sensor was tested in the presence of 0.5 mM glucose solution each day, after 30 days, the response of the sensor decreased 9.6% compared to the initial response, that shows the sensors have long-term stability.

Some species that usually existed and possibly interfered determination of glucose such as dopamine (DA), uric acid (UA) and p-acetamidophenol (AP) were investigated. When 0.5 mM AA, 0.5 mM UA, and 0.5 mM AP was added into 1.0 mM glucose solution, the changes in ECL signal generated from DA, UA and AP was negligible. The result revealed that the glucose biosensor has a good anti-interferent ability, which may be attributed to the enzymatic substrate-specific reaction.

3.6. Recovery experiment

The applicability of the biosensor was estimated by standard addition method. Table S1 listed the recovery of different

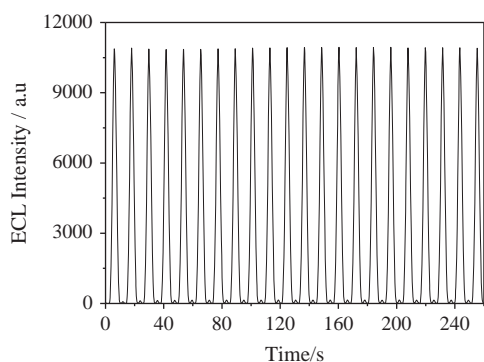


Fig. 4. The ECL stability of GOD/Au_{shell}@GOD/CS/GCE sensor to 3.31 mM glucose in pH 7.4 PBS with 0.1 mM luminol.

Table 1
Recoveries of glucose by the biosensor.

Sample	$C_{\text{Original}}/\mu\text{M}$	$C_{\text{Added}}/\mu\text{M}$	$C_{\text{Found}}^{\text{a}}/\mu\text{M}$	R.S.D./%	Recovery/%
1	50	5	56.56 ± 1.9	3.4	102.8
2	200	50	259.3 ± 6.8	2.6	103.7
3	500	50	534.1 ± 22.3	4.2	97.0
4	800	50	827.4 ± 35.5	4.3	97.3

^a Mean value \pm standard deviation (S.D.) of three measurements.

cholesterol concentrations. The recovery rate was between 97.0% and 103.7% (See Table 1). The results proved that the biosensor had a potential for practical application.

4. Conclusions

In conclusion, hollow gold nanospheres (Au_{shell}@GOD) were synthesized via a method of glucose oxidase (GOD) cross-linked with glutaraldehyde as a template. An electrogenerated chemiluminescence glucose biosensor was constructed based on the Au_{shell}@GOD nanoparticles. The prepared biosensor exhibited good performance that may benefit from the following: firstly, the prepared hollow Au_{shell}@GOD nanoparticles have a large surface area, high conductivity, good biocompatibility, which could effectively increase the loading of GOD and keep the biological activity of GOD. Thus, GOD molecules can exist inside and outside of Au_{shell}, which could effectively amplify the ECL intensity of luminol-H₂O₂ system. Secondly, the Au_{shell} assembling on the electrode can catalyze the electro-oxidization of luminol, and the stronger ECL signal was obtained in neutral aqueous solution. Such fabrication of biosensor exhibited good performance. The Au_{shell}@GOD nanoparticles could have potential applications in biotechnology and clinical diagnosis.

Acknowledgments

This work was supported by the National Natural Science Foundation of China (21275119, 21075100), the Ministry of Education of the People's Republic of China (Project 708073), the Nature Science Foundation of Chongqing City (CSTC-2011BA7003 and CSTC-2009BA1003), the Specialized Research Fund for the Doctoral Program of Higher Education (20100182110015), the Doctor Foundation of Southwest University (swu113029), and the Fundamental Research Funds for the Central Universities (XDJK2013C115) and (XDJK2013A008).

References

- [1] A.W. Knight, G.M. Greenway, *Analyst* 119 (1994) 879–890.
- [2] W.J. Miao, *Chem. Rev.* 108 (2008) 2506–2553.
- [3] Z. Chang, J.M. Zhou, K. Zhao, N.N. Zhu, P.G. He, Y.Z. Fang, *Electrochim. Acta* 52 (2006) 575–580.
- [4] Y.B. Li, Z.J. Zhang, J.S. Li, H.G. Li, Y. Chen, Z.H. Liu, *Talanta* 84 (2011) 690–695.
- [5] S.J. Xu, Y. Liu, T.H. Wang, J.H. Li, *Anal. Chem.* 83 (2011) 3817–3823.
- [6] H. Dai, Y.W. Chi, X.P. Wu, Y.M. Wang, M.D. Wei, G.N. Chen, *Biosens. Bioelectron.* 25 (2010) 1414–1419.
- [7] Z.Y. Lin, J.J. Sun, J.H. Chen, L. Guo, Y.T. Chen, G.N. Chen, *Anal. Chem.* 80 (2008) 2826–2831.
- [8] L.H. Zhang, Z.A. Xu, X.P. Sun, S.J. Dong, *Biosens. Bioelectron.* 22 (2007) 1097–1100.
- [9] M.H. Zhang, R. Yuan, Y.Q. Chai, S.H. Chen, H.A. Zhong, C. Wang, Y.F. Cheng, *Biosens. Bioelectron.* 32 (2012) 288–292.
- [10] Z. Zhao, X.M. Zhou, D. Xing, *Biosens. Bioelectron.* 31 (2012) 299–304.
- [11] H.O. Albrecht, *Z. Phys. Chem.* 136 (1928) 321–330.
- [12] B. Qiu, Z.Y. Lin, J. Wang, Z.H. Chen, J.H. Chen, G.N. Chen, *Talanta* 78 (2009) 76–80.
- [13] T. Ren, J.Z. Xu, Y.F. Tu, S. Xu, J.J. Zhu, *Electrochem. Commun.* 7 (2005) 5–9.
- [14] X.M. Chen, Z.J. Lin, Z.M. Cai, X. Chen, M. Oyama, X.R. Wang, *J. Nanosci. Nanotechnol.* 9 (2009) 2413–2420.

- [15] B. Haghighia, S. Bozorgzadeha, L. Gortonb, *Sensors Actuat. B.* 155 (2011) 577–583.
- [16] B. Haghighi, S. Bozorgzadeh, *Anal. Chim. Acta* 697 (2011) 90–97.
- [17] Q. Li, J.Y. Zheng, Y.L. Yan, Y.S. Zhao, J.N. Yao, *Adv. Mater.* 24 (2012) 4745–4749.
- [18] S.N. Ding, B.H. Gao, D. Shan, Y.M. Sun, S. Cosnier, *Biosens. Bioelectron.* 39 (2013) 342–345.
- [19] R. Cui, Y.P. Gu, L. Bao, J.Y. Zhao, B.P. Qi, Z.L. Zhang, Z.X. Xie, D.W. Pang, *Anal. Chem.* 84 (2012) 8932–8935.
- [20] Y.L. Cao, R. Yuan, Y.Q. Chai, Li. Mao, H. Niu, H.J. Liu, Y. Zhuo, *Biosens. Bioelectron.* 31 (2012) 305–309.
- [21] D.Y. Tian, C.F. Duan, W. Wang, H. Cui, *Biosens. Bioelectron.* 25 (2010) 2290–2295.
- [22] W. Wang, Y.P. Dong, H. Cui, Y. Xu, *Langmuir* 23 (2007) 523–529.
- [23] A.J. Amali, N.H. Awwad, R.K. Rana, D. Patra, *Anal. Chim. Acta* 708 (2011) 75–83.
- [24] D. Patra, R. Aridi, K. Bouhadir, *Microchim. Acta* 180 (2013) 59–64.
- [25] D. Patra, F. Sleem, *Anal. Chim. Acta* 795 (2013) 60–68.
- [26] D. Patra, A.J. Amali, R.K. Rana, *J. Mater. Chem.* 19 (2009) 4017–4021.
- [27] R. Kumar, A.N. Maitra, P.K. Patanjali, P. Sharma, *Biomaterials* 26 (2005) 6743–6753.
- [28] J. Zhou, F. Ren, W. Wu, S.F. Zhang, X.H. Xiao, J.X. Xu, C.Z. Jiang, *J. Colloid Interface Sci.* 387 (2012) 47–55.
- [29] A. Manna, T. Imae, T. Yogo, K. Aoi, M. Okazaki, *J. Colloid Interface Sci.* 256 (2002) 297–303.